

Closing the Boundary Layer Energy and Water Budgets with a Little MAGIC

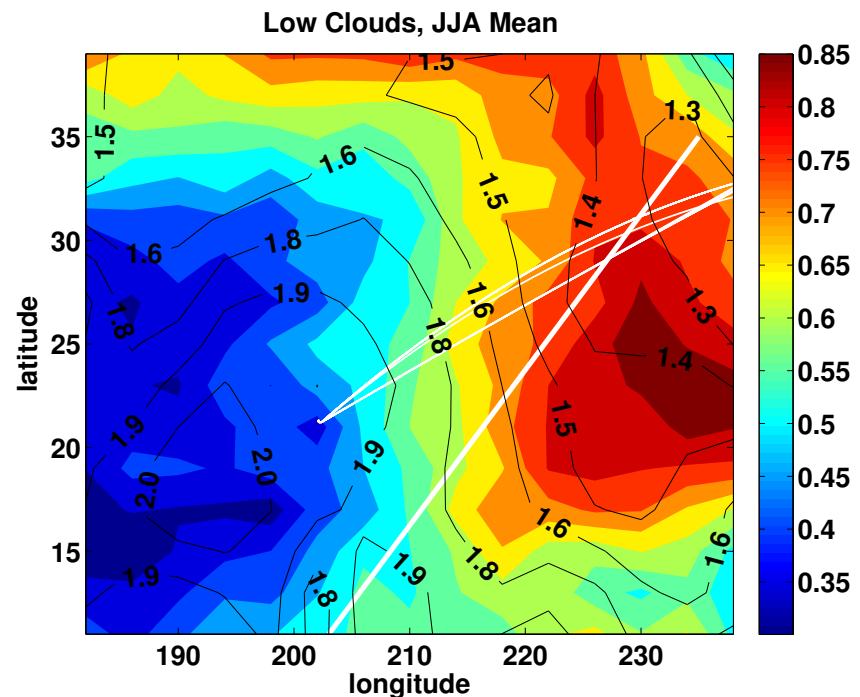
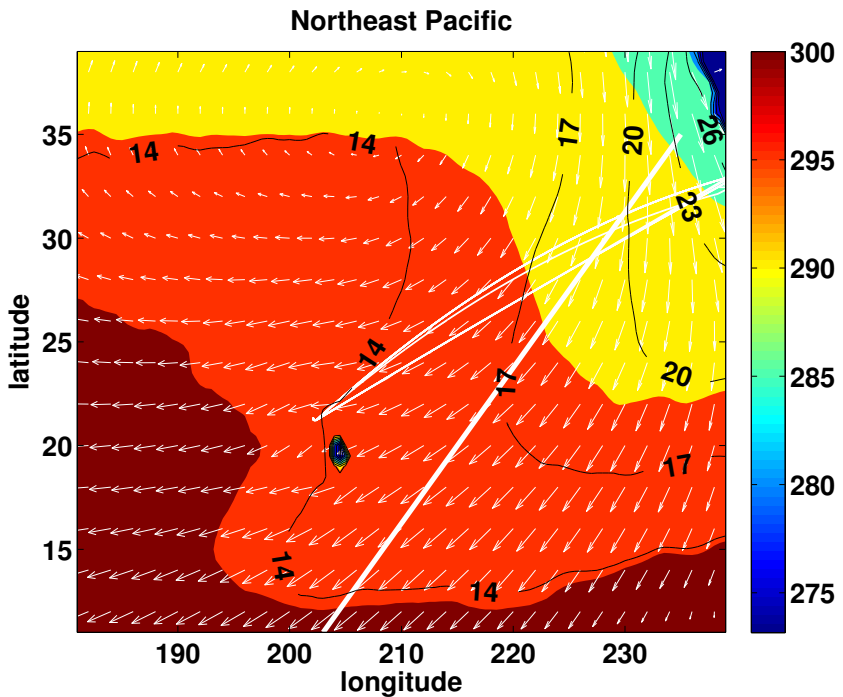
Peter Kalmus, Matt Lebsack, João Teixeira
JPL/Caltech
First MAGIC Science Workshop
May 6, 2014



National Aeronautics and Space Administration
Jet Propulsion Laboratory
California Institute of Technology
Pasadena, California
(c) 2014 California Institute of Technology.
Government sponsorship acknowledged.

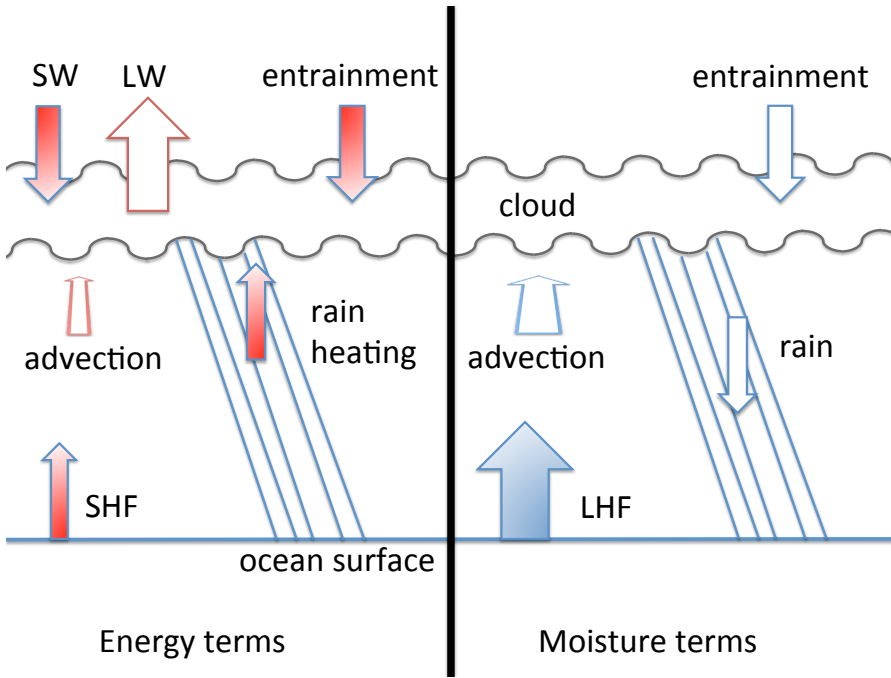
GPCI Transect

Transition from stratocumulus to trade cumulus



Subtropical marine stratocumulus regions might be an important lever in the climate system. Regional energy and water budgets could provide a holistic test for observations & models.

Energy and Water Budgets



$$\langle \bar{\rho} \rangle c_p h \frac{\partial \langle \bar{\theta}_l \rangle}{\partial t} = -c_p h \langle \bar{\rho} \bar{v} \cdot \nabla_H \bar{\theta}_l \rangle + \text{SHF} - L F_p(0) + \bar{\rho}|_h c_p w_e \Delta \theta_l + \langle \bar{\rho} \rangle c_p \left(\langle \bar{\theta}_l \rangle - \bar{\theta}_l|_{h_-} \right) \bar{v}|_h \cdot \nabla_H h - \Delta_{BL} (F_{SW} + F_{LW})$$

$$\langle \bar{\rho} \rangle L h \frac{\partial \langle \bar{q}_t \rangle}{\partial t} = -L h \langle \bar{\rho} \bar{v} \cdot \nabla_H \bar{q}_t \rangle + \text{LHF} + L F_p(0) + \bar{\rho}|_h L w_e \Delta q_t + \langle \bar{\rho} \rangle L \left(\langle \bar{q}_t \rangle - \bar{q}_t|_{h_-} \right) \bar{v}|_h \cdot \nabla_H h$$

$$\Delta_{BL} F = F(h) - F(0)$$

$$\Delta A \equiv [\bar{A}|_{h+} - \langle \bar{A} \rangle]$$

h is BL height

Ingredients in the budgets

Observational

MAGIC, COSMIC, CloudSat, CALIPSO, Aqua (MODIS)

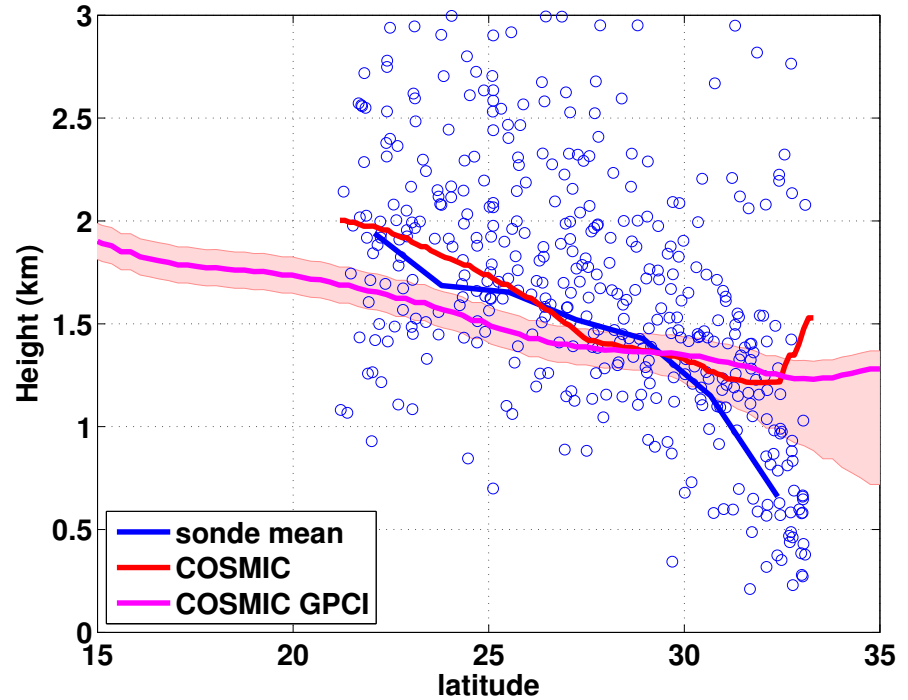
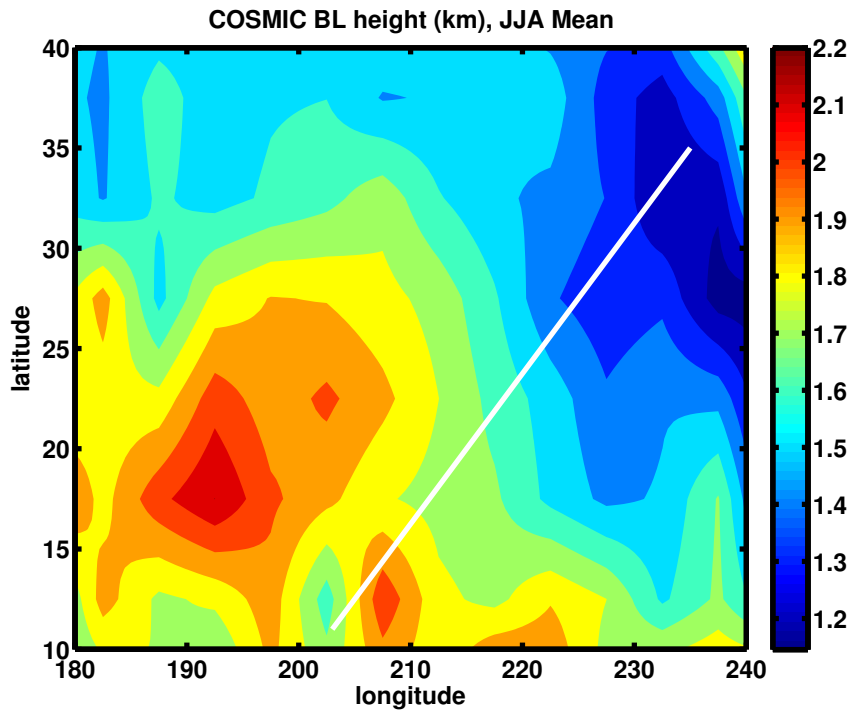
Reanalysis

ECMWF ERA-Interim

For uncertainty estimation

GPCP, CERES, NCEP

Boundary Layer Height (BLH)



COSMIC radio occultation data (JJA)

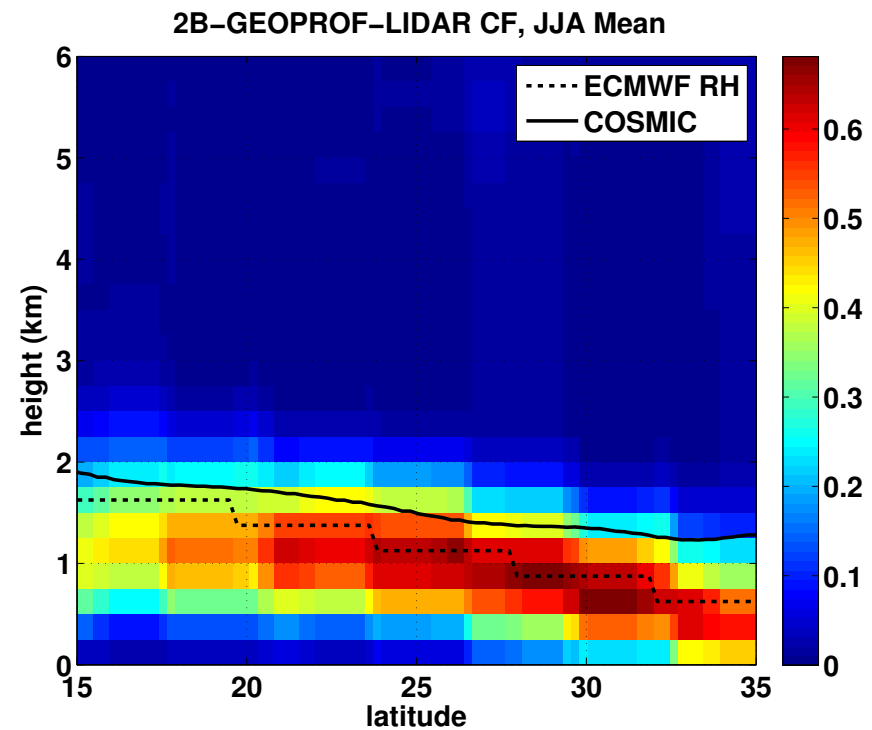
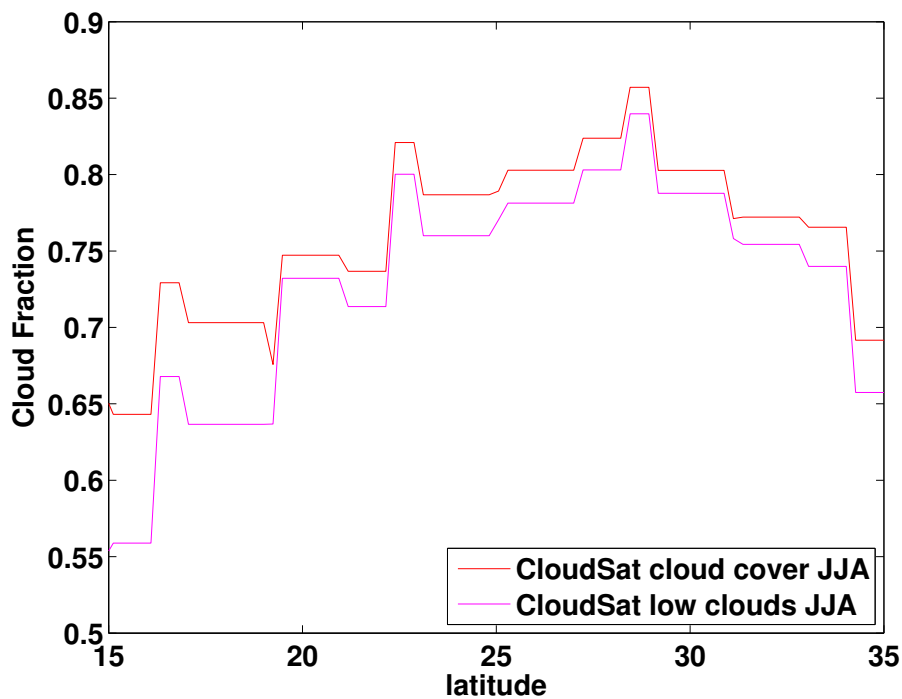
MAGIC radiosonde profiles (JJA) – estimate inversion heights from RH profiles

Estimated coast bias error by matching COSMIC to MAGIC on distance-from-coast basis

Probably caused by COSMIC 5° resolution and the Sierra Nevada

Affects advection, entrainment, radiation terms

Cloud Fraction

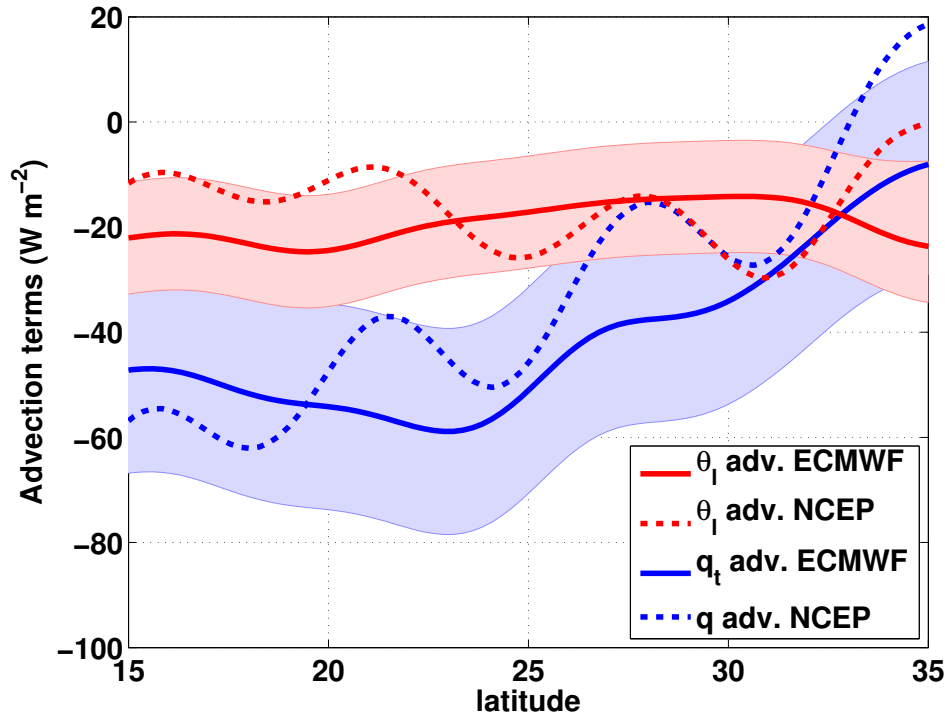


Low clouds: up to 680 hPa (about 3.4 km).
2B-GEOPROF-LIDAR product (Mace et al. 2009)

Horizontal Advection

ECMWF ERA-Interim

RMS uncertainty estimated from NCEP reanalysis of θ -advection (dotted red line)

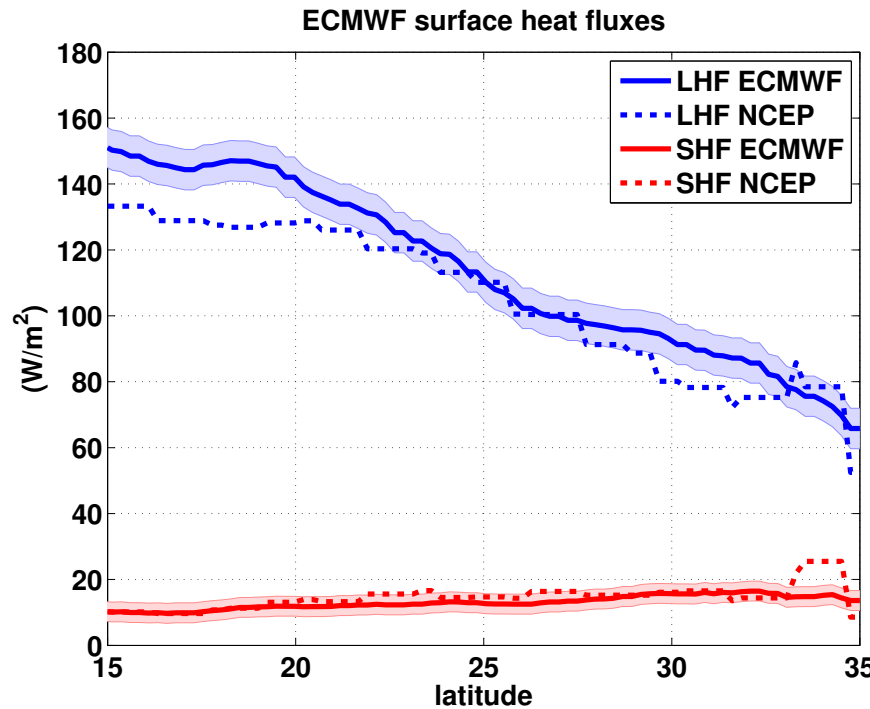


$$\langle \bar{\rho} \rangle c_p h \frac{\partial \langle \bar{\theta}_l \rangle}{\partial t} = -c_p h \langle \bar{\rho} \bar{v} \cdot \nabla_H \bar{\theta}_l \rangle + \text{SHF} - LF_p(0) + \bar{\rho}|_h c_p w_e \Delta \theta_l + \langle \bar{\rho} \rangle c_p \left(\langle \bar{\theta}_l \rangle - \bar{\theta}_l|_{h_-} \right) \bar{v}|_h \cdot \nabla_H h - \Delta_{BL}(F_{SW} + F_{LW})$$

$$\langle \bar{\rho} \rangle L h \frac{\partial \langle \bar{q}_t \rangle}{\partial t} = -L h \langle \bar{\rho} \bar{v} \cdot \nabla_H \bar{q}_t \rangle + \text{LHF} + LF_p(0) + \bar{\rho}|_h L w_e \Delta q_t + \langle \bar{\rho} \rangle L \left(\langle \bar{q}_t \rangle - \bar{q}_t|_{h_-} \right) \bar{v}|_h \cdot \nabla_H h$$

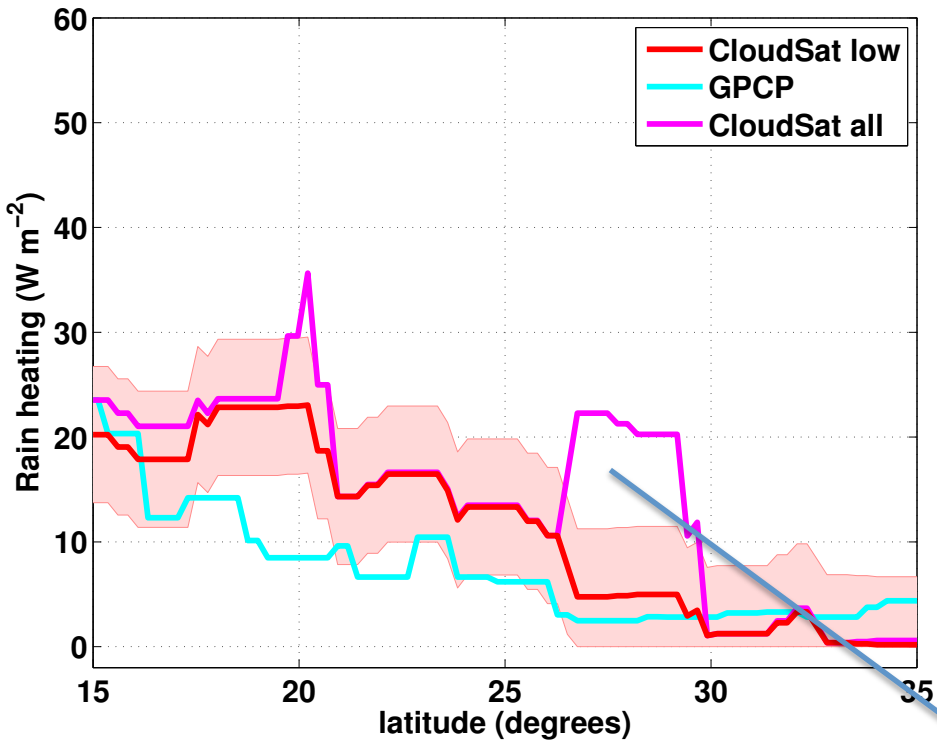
Surface Fluxes

ECMWF ERA-Interim with RMS uncertainty from NCEP.



$$\begin{aligned} \langle \bar{\rho} \rangle c_p h \frac{\partial \langle \bar{\theta}_l \rangle}{\partial t} &= -c_p h \langle \bar{\rho} \bar{\mathbf{v}} \cdot \nabla_H \bar{\theta}_l \rangle + \text{SHF} - LF_p(0) + \bar{\rho} \Big|_h c_p w_e \Delta \theta_l + \langle \bar{\rho} \rangle c_p \left(\langle \bar{\theta}_l \rangle - \bar{\theta}_l \Big|_{h_-} \right) \bar{\mathbf{v}} \Big|_h \cdot \nabla_H h - \Delta_{\text{BL}} (F_{\text{SW}} + F_{\text{LW}}) \\ \langle \bar{\rho} \rangle L h \frac{\partial \langle \bar{q}_t \rangle}{\partial t} &= -L h \langle \bar{\rho} \bar{\mathbf{v}} \cdot \nabla_H \bar{q}_t \rangle + \text{LHF} + LF_p(0) + \bar{\rho} \Big|_h L w_e \Delta q_t + \langle \bar{\rho} \rangle L \left(\langle \bar{q}_t \rangle - \bar{q}_t \Big|_{h_-} \right) \bar{\mathbf{v}} \Big|_h \cdot \nabla_H h \end{aligned}$$

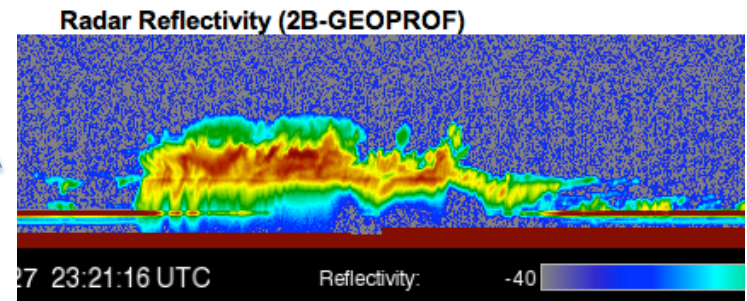
Rain



Low rain is rain from cloud tops up to 680 hPa (about 3.4 km).
2C-PRECIP-COLUMN product (Lebsack et al. 2011).

We cut high rain (storms).

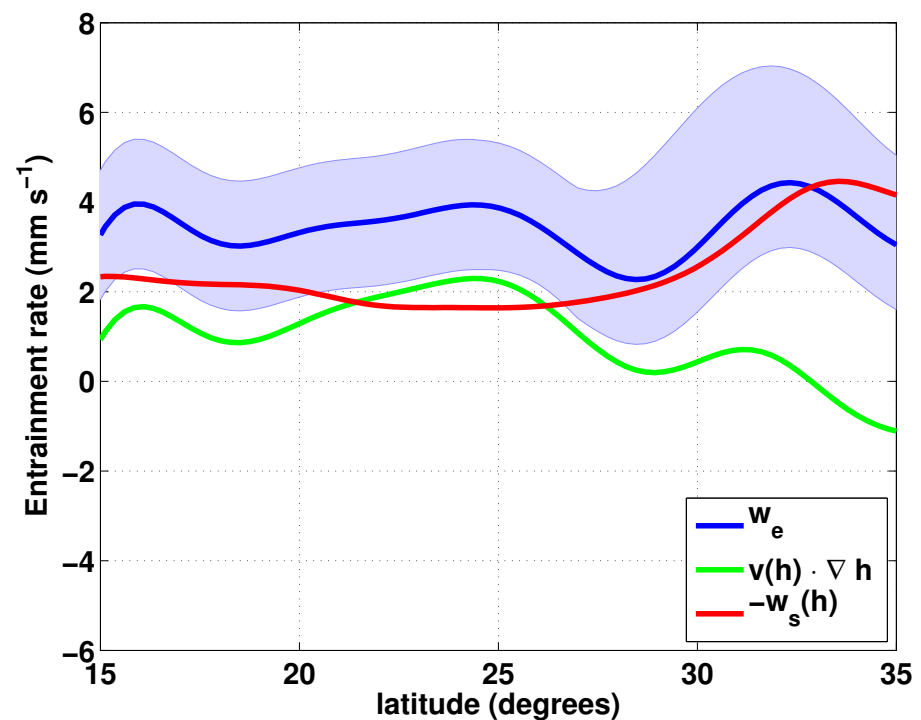
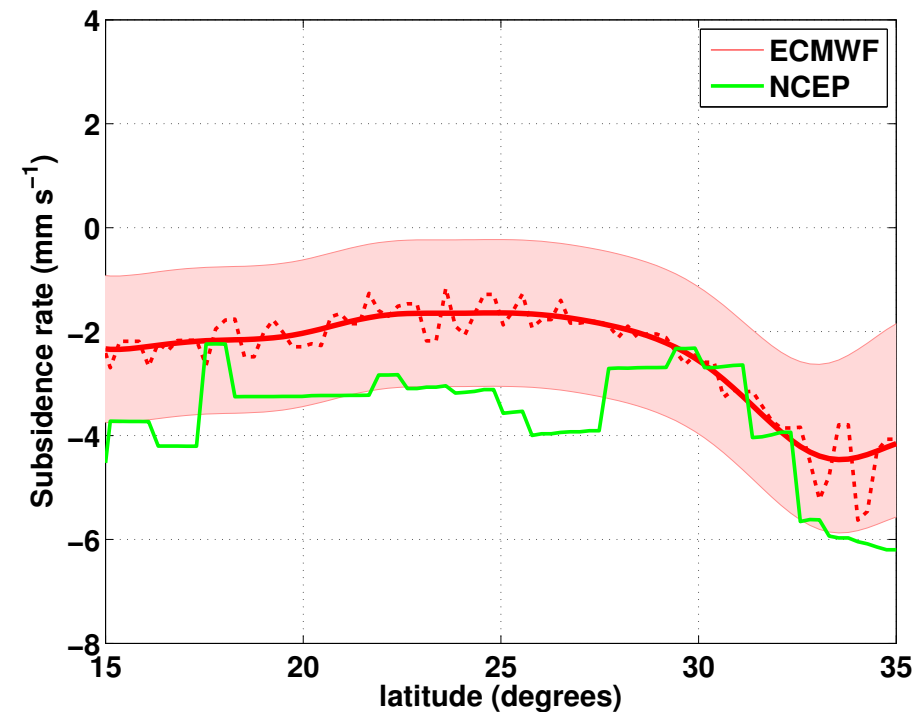
Uncertainty estimated from GPCP.



$$\langle \bar{\rho} \rangle c_p h \frac{\partial \langle \bar{\theta}_l \rangle}{\partial t} = -c_p h \langle \bar{\rho} \bar{v} \cdot \nabla_H \bar{\theta}_l \rangle + \text{SHF} - LF_p(0) + \bar{\rho}|_h c_p w_e \Delta \theta_l + \langle \bar{\rho} \rangle c_p \left(\langle \bar{\theta}_l \rangle - \bar{\theta}_l|_{h_-} \right) \bar{v}|_h \cdot \nabla_H h - \Delta_{BL}(F_{SW} + F_{LW})$$

$$\langle \bar{\rho} \rangle L h \frac{\partial \langle \bar{q}_t \rangle}{\partial t} = -L h \langle \bar{\rho} \bar{v} \cdot \nabla_H \bar{q}_t \rangle + \text{LHF} + LF_p(0) + \bar{\rho}|_h L w_e \Delta q_t + \langle \bar{\rho} \rangle L \left(\langle \bar{q}_t \rangle - \bar{q}_t|_{h_-} \right) \bar{v}|_h \cdot \nabla_H h$$

Subsidence, Entrainment



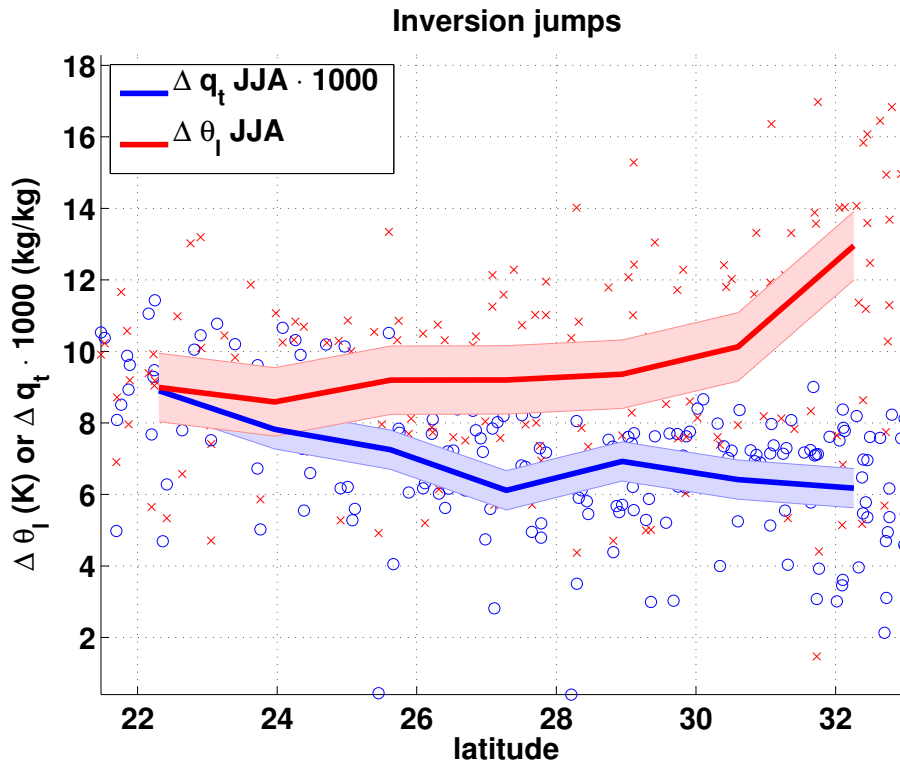
$$\bar{w}_e = \bar{\mathbf{u}(h)} \cdot \bar{\nabla h} - \bar{w}_s(h).$$

Low-pass filter applied to remove low-frequency noise
red dotted line is before filtering

Subregion	Latitude	$\overline{w_e}$ (mm s ⁻¹)	$\overline{w_s}$ (mm s ⁻¹)	$\overline{\mathbf{v}(h) \cdot \nabla h}$ (mm s ⁻¹)	\bar{h} (km)
NE Pacific	15°N–35°N	$3.4^{+1.6}_{-1.4}$	$2.5^{+1.5}_{-1.4}$	$1.0^{+0.8}_{-0.1}$	$1.5^{+0.1}_{-0.2}$
	25°N–35°N	$3.3^{+1.8}_{-1.4}$	$3.0^{+1.6}_{-1.4}$	$0.4^{+1.4}_{-0.1}$	$1.3^{+0.1}_{-0.2}$
	15°N–25°N	3.5 ± 1.4	1.9 ± 1.4	1.6 ± 0.2	1.7 ± 0.1
WB2004	25°N–35°N	4.8 ± 1.2	4.1 ± 0.8	0.8 ± 0.2	1.2 ± 0.1
WB2004	15°N–25°N	3.2 ± 0.8	2.1 ± 0.4	1.1 ± 0.3	1.7 ± 0.3

WB2004= Wood & Bretherton 2004

Cross-inversion jumps



$$\Delta A \equiv [\bar{A}|_{h+} - \langle \bar{A} \rangle]$$

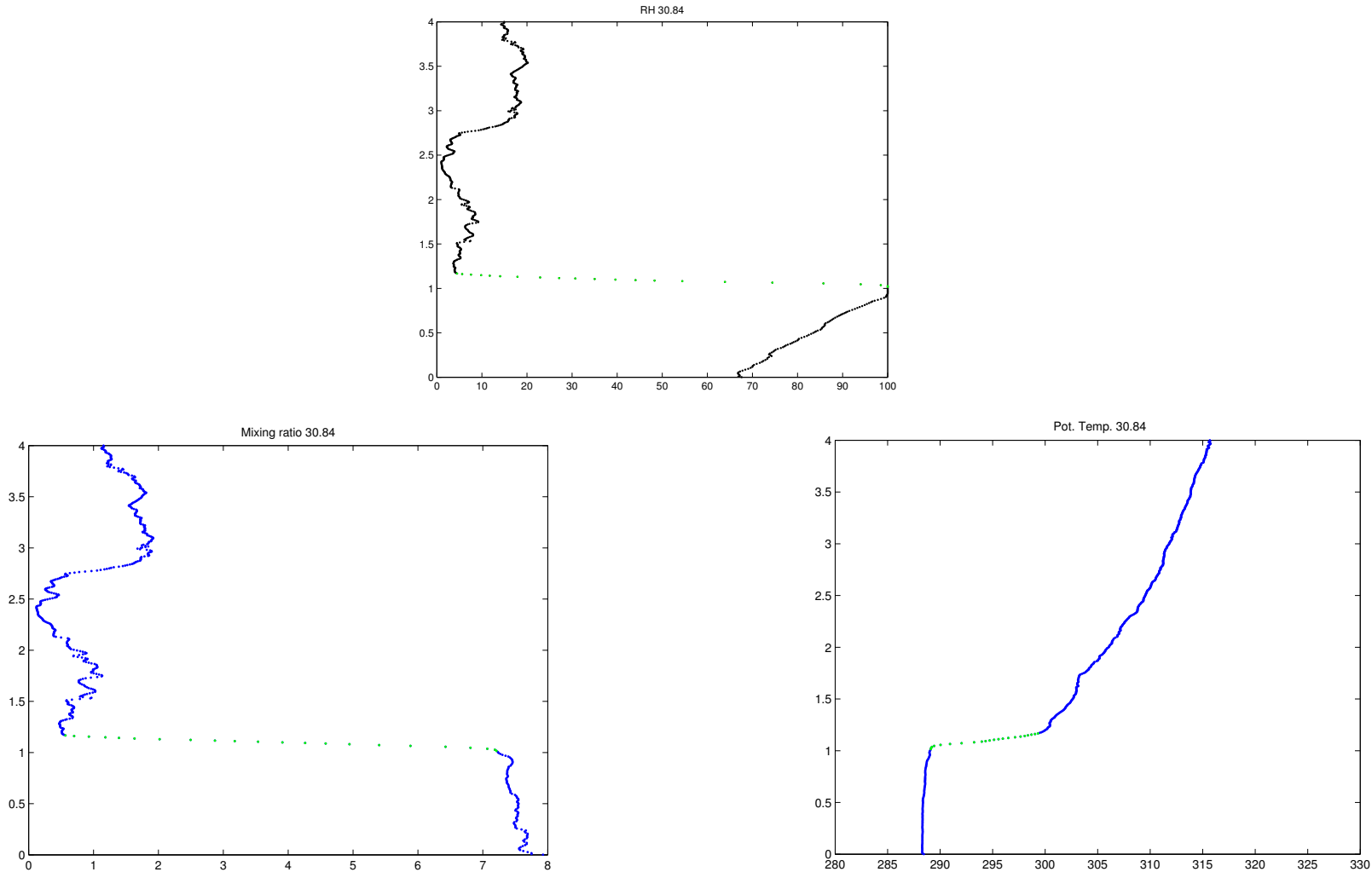
From MAGIC radiosondes.

Uncertainty estimates are from examination of individual jumps.

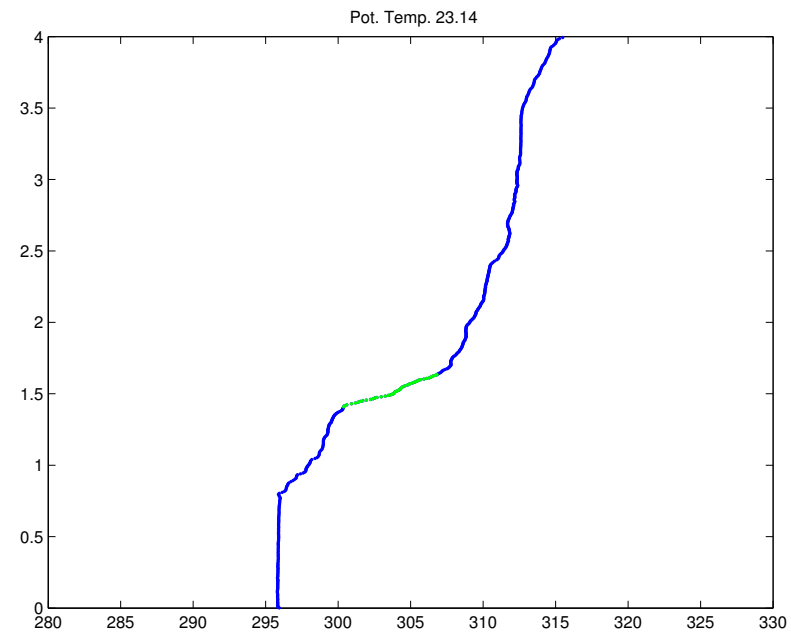
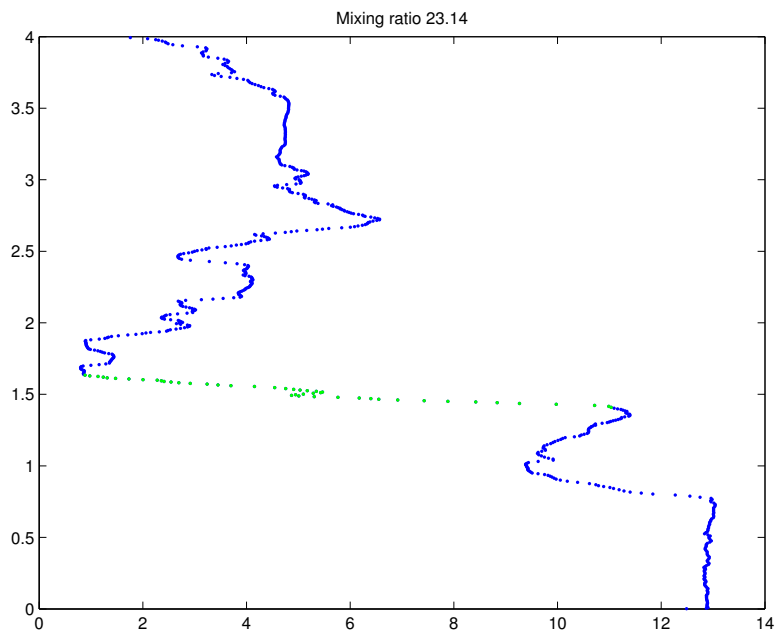
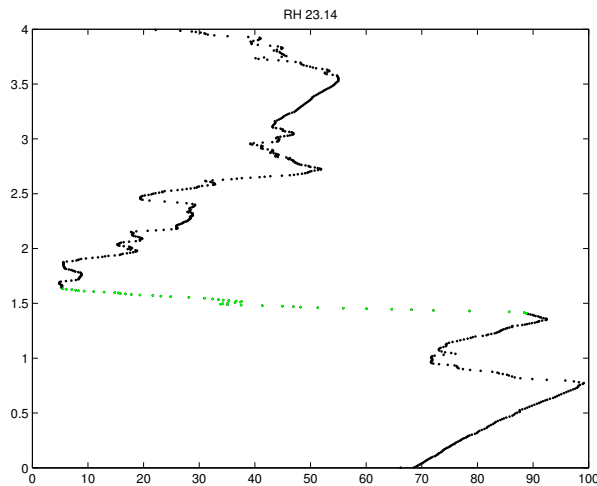
$$\langle \bar{\rho} \rangle c_p h \frac{\partial \langle \bar{\theta}_l \rangle}{\partial t} = -c_p h \langle \bar{\rho} \bar{\mathbf{v}} \cdot \nabla_H \bar{\theta}_l \rangle + \text{SHF} - LF_p(0) + \bar{\rho}|_h c_p w_e \Delta\theta_l + \langle \bar{\rho} \rangle c_p \left(\langle \bar{\theta}_l \rangle - \bar{\theta}_l|_{h_-} \right) \bar{\mathbf{v}}|_h \cdot \nabla_H h - \Delta_{\text{BL}}(F_{\text{SW}} + F_{\text{LW}})$$

$$\langle \bar{\rho} \rangle L h \frac{\partial \langle \bar{q}_t \rangle}{\partial t} = -L h \langle \bar{\rho} \bar{\mathbf{v}} \cdot \nabla_H \bar{q}_t \rangle + \text{LHF} + LF_p(0) + \bar{\rho}|_h L w_e \Delta q_t + \langle \bar{\rho} \rangle L \left(\langle \bar{q}_t \rangle - \bar{q}_t|_{h_-} \right) \bar{\mathbf{v}}|_h \cdot \nabla_H h$$

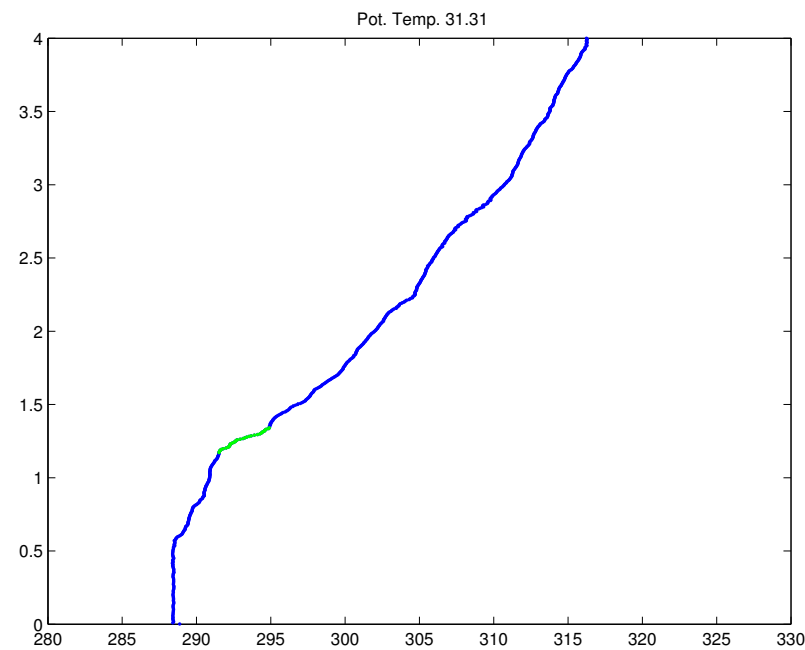
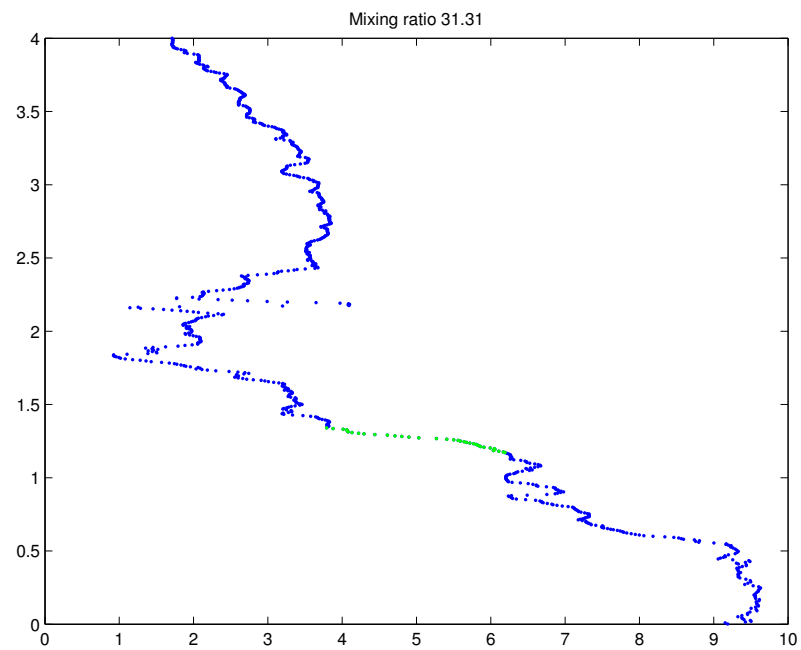
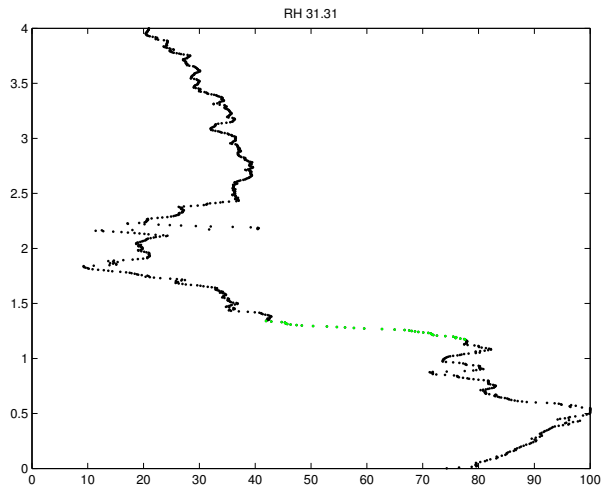
Cross-inversion jumps



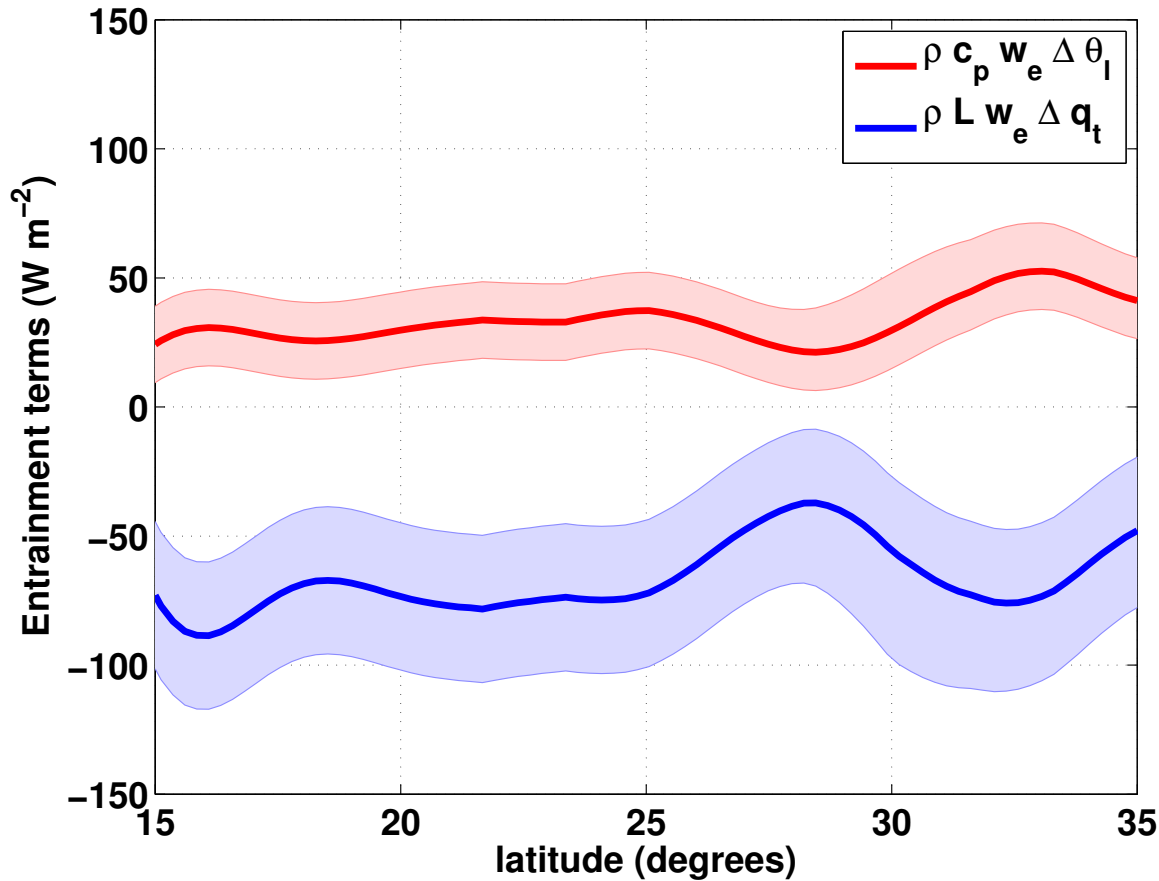
Cross-inversion jumps



Cross-inversion jumps



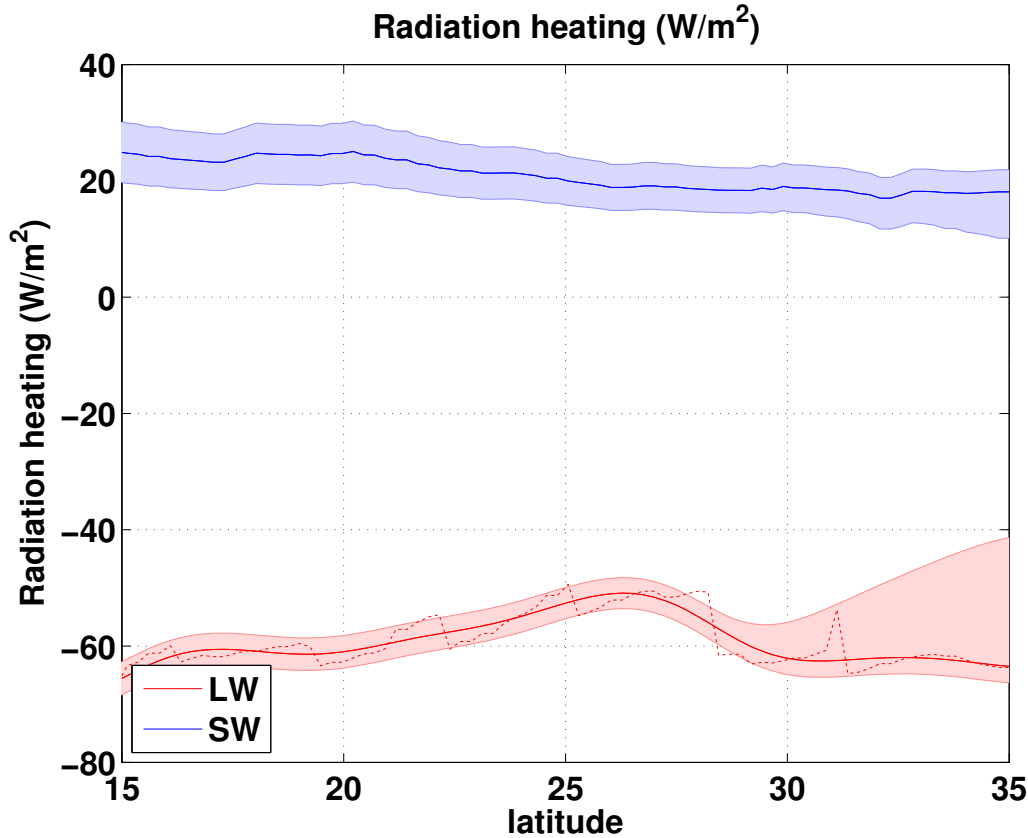
Entrainment of q_t and θ_l



$$\langle \bar{\rho} \rangle c_p h \frac{\partial \langle \bar{\theta}_l \rangle}{\partial t} = -c_p h \langle \bar{\rho} \bar{\mathbf{v}} \cdot \nabla_H \bar{\theta}_l \rangle + \text{SHF} - LF_p(0) + \bar{\rho}|_h c_p w_e \Delta \theta_l + \langle \bar{\rho} \rangle c_p \left(\langle \bar{\theta}_l \rangle - \bar{\theta}_l|_{h_-} \right) \bar{\mathbf{v}}|_h \cdot \nabla_H h - \Delta_{\text{BL}} (F_{\text{SW}} + F_{\text{LW}})$$

$$\langle \bar{\rho} \rangle L h \frac{\partial \langle \bar{q}_t \rangle}{\partial t} = -L h \langle \bar{\rho} \bar{\mathbf{v}} \cdot \nabla_H \bar{q}_t \rangle + \text{LHF} + LF_p(0) + \bar{\rho}|_h L w_e \Delta q_t + \langle \bar{\rho} \rangle L \left(\langle \bar{q}_t \rangle - \bar{q}_t|_{h_-} \right) \bar{\mathbf{v}}|_h \cdot \nabla_H h$$

Radiation



2B-FLXHR-LIDAR product
(Henderson et al. 2013).

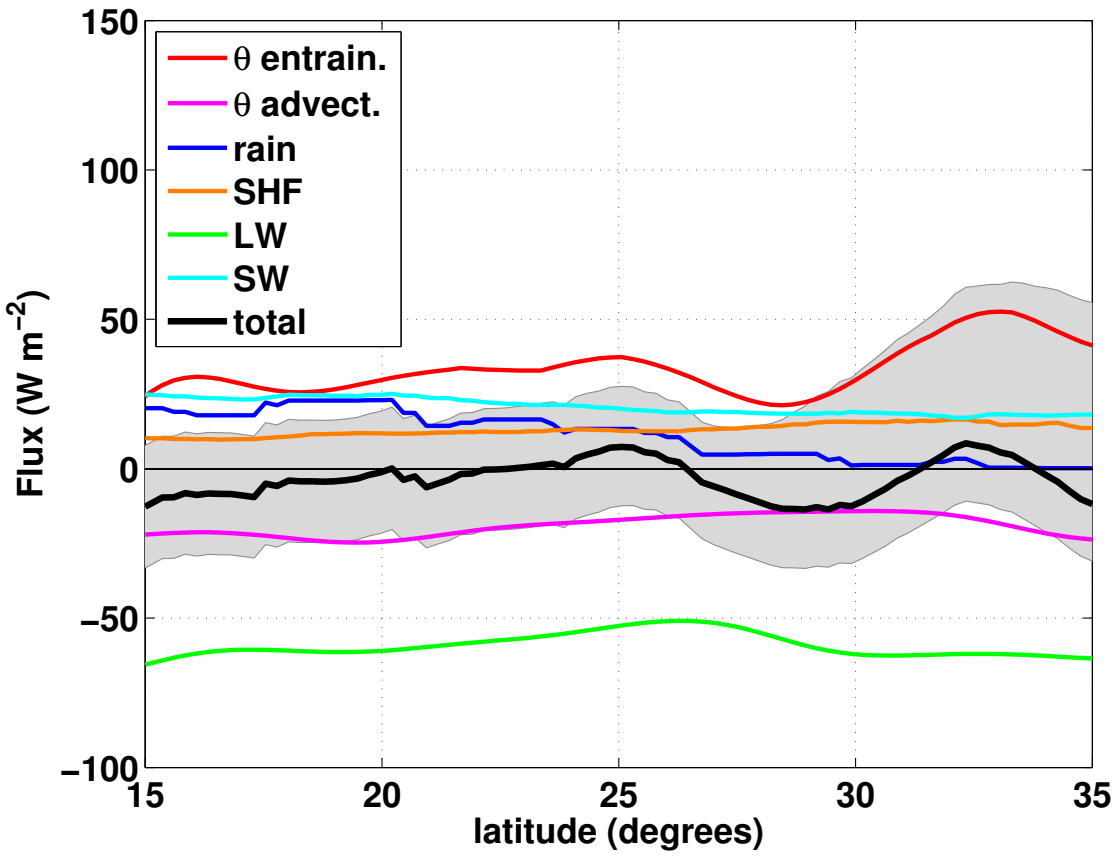
Uncertainty estimates from
TOA comparisons with CERES
(Henderson et al. 2013).

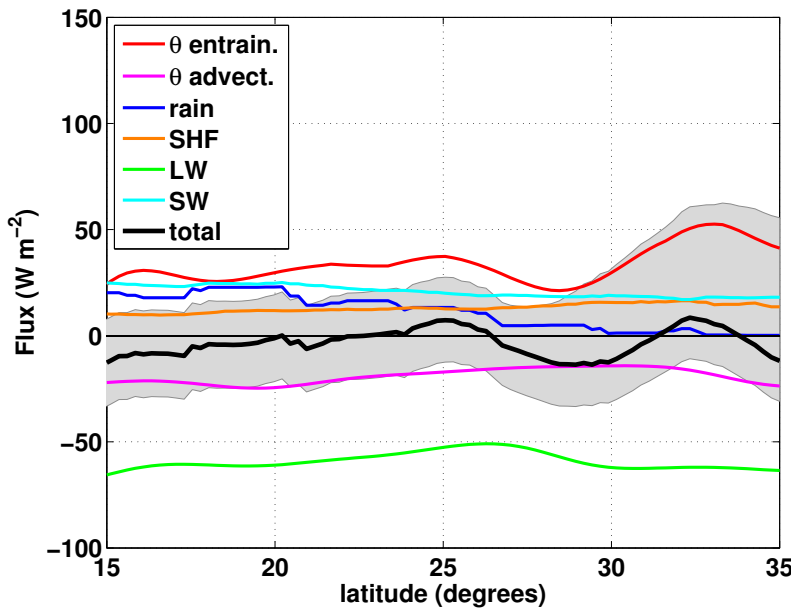
$$\Delta_{BL}F = F(h) - F(0).$$

$$\langle \bar{\rho} \rangle c_p h \frac{\partial \langle \bar{\theta}_l \rangle}{\partial t} = -c_p h \langle \bar{\rho} \bar{v} \cdot \nabla_H \bar{\theta}_l \rangle + \text{SHF} - LF_p(0) + \bar{\rho}|_h c_p w_e \Delta \theta_l + \langle \bar{\rho} \rangle c_p \left(\langle \bar{\theta}_l \rangle - \bar{\theta}_l|_{h_-} \right) \bar{v}|_h \cdot \nabla_H h - \Delta_{BL}(F_{SW} + F_{LW})$$

$$\langle \bar{\rho} \rangle L h \frac{\partial \langle \bar{q}_t \rangle}{\partial t} = -L h \langle \bar{\rho} \bar{v} \cdot \nabla_H \bar{q}_t \rangle + \text{LHF} + LF_p(0) + \bar{\rho}|_h L w_e \Delta q_t + \langle \bar{\rho} \rangle L \left(\langle \bar{q}_t \rangle - \bar{q}_t|_{h_-} \right) \bar{v}|_h \cdot \nabla_H h$$

Energy Budget



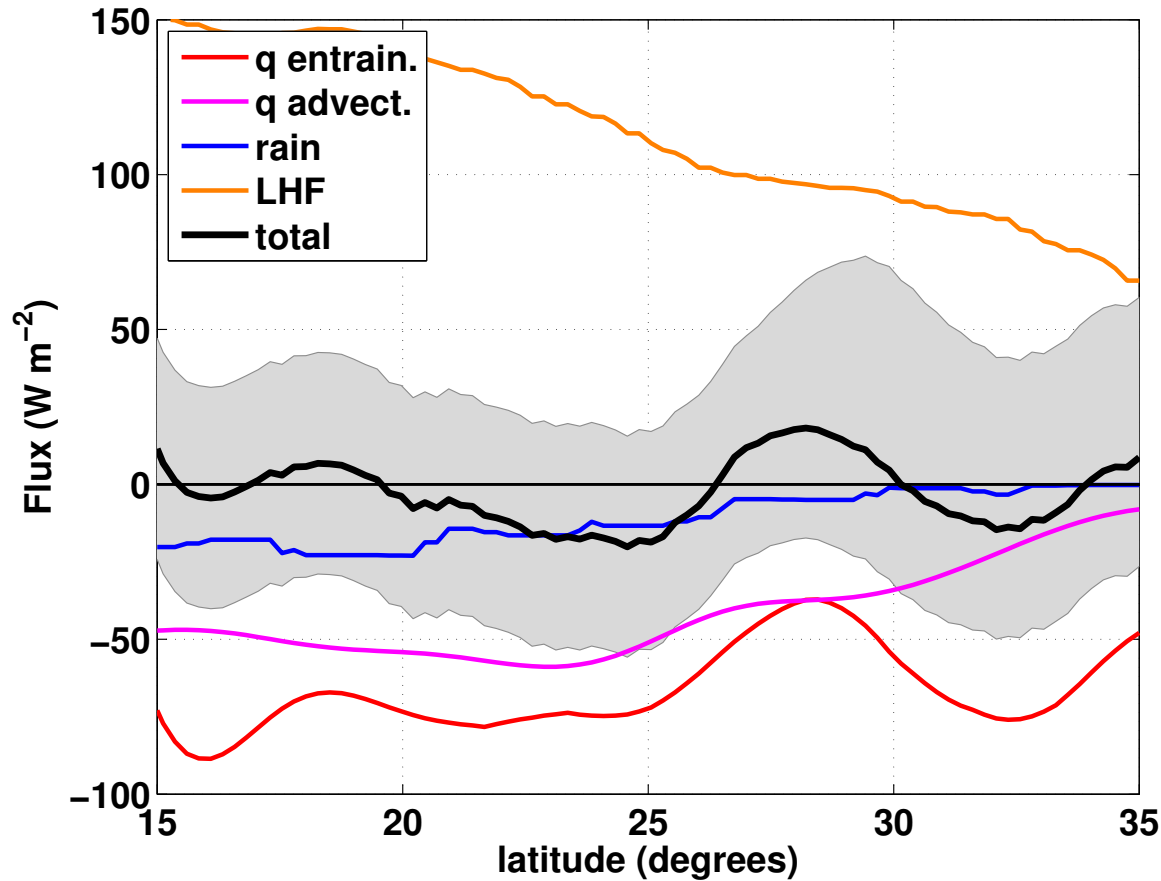


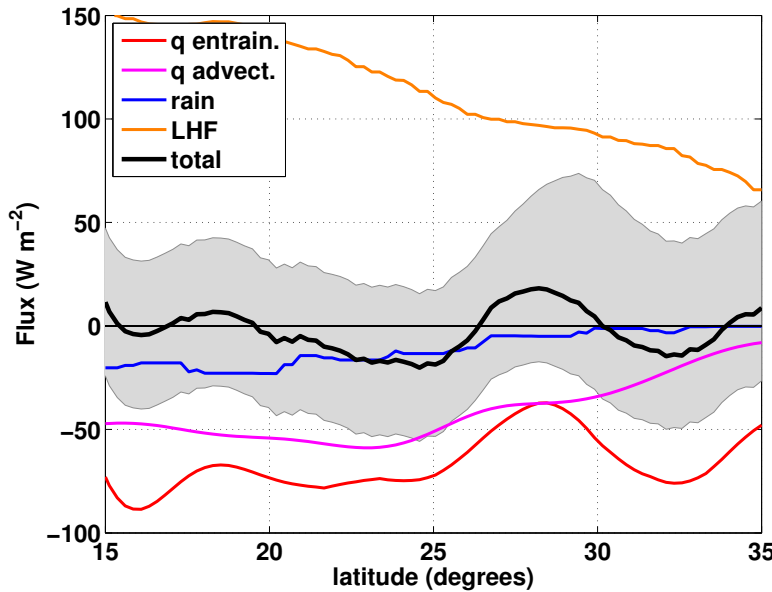
Small increases in rain heating (15 Wm^{-2}) and SW (5 Wm^{-2}) balanced by decreasing entrainment heating (-6 Wm^{-2}), increasing advective cooling (-4 Wm^{-2}), and decreased mixing (-5 Wm^{-2})

Caldwell et al. 2005 (CBW2005) was a six day ship-based experiment in the SE Pacific.

Regime/study	$-c_p h \langle \bar{\rho} \bar{\mathbf{v}} \cdot \nabla_H \bar{\theta}_l \rangle$	SHF	$-LF_p(0)$	-SW	-LW	$\bar{\rho} _h c_p w_e \Delta \theta_l$	$\bar{\mathbf{v}} _h \cdot \nabla_H h$	residual
15°N–35°N	-19 ± 11	13 ± 3	11^{+6}_{-5}	21^{+4}_{-5}	-59^{+6}_{-3}	34^{+16}_{-15}	-4	-3^{+31}_{-20}
25°N–35°N	-17^{+12}_{-11}	15 ± 3	3^{+6}_{-3}	18^{+4}_{-5}	-59^{+9}_{-3}	36^{+18}_{-15}	-1	-4^{+42}_{-19}
15°N–25°N	-21 ± 11	12 ± 3	18 ± 6	23 ± 5	-59 ± 3	31 ± 15	-6	-2 ± 20
30°N–35°N	-18	15	1	18	-62	46	0	0
25°N–30°N	-15	14	6	19	-55	27	-2	-7
20°N–25°N	-20	12	15	22	-56	34	-7	1
15°N–20°N	-23	11	21	24	-61	28	-5	-5
CBW2005	-19 ± 3	14 ± 1	5 ± 1	26 ± 1	-78 ± 1	41 ± 6		-11

Water Budget





Increasing evaporation balanced
in roughly equal parts by
entrainment drying, rain, and
horizontal advection.

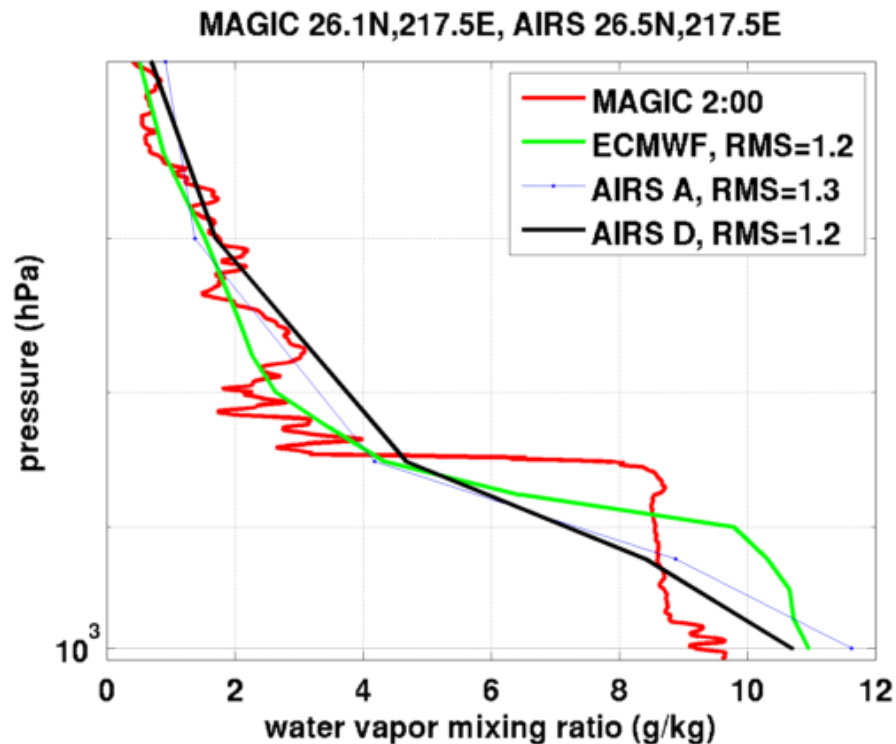
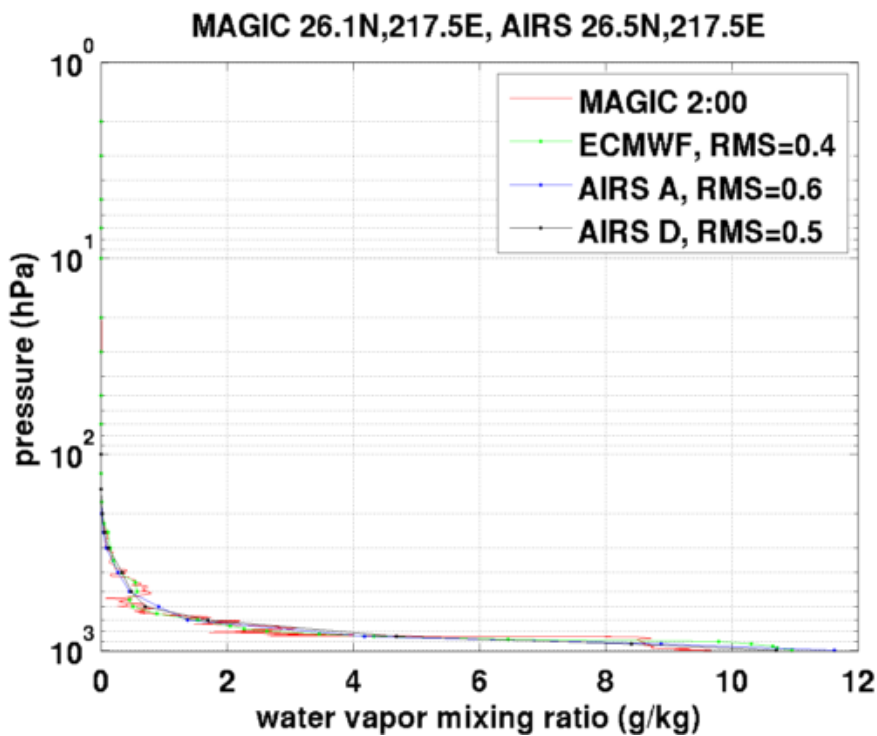
Regime/study	$-Lh\langle\bar{\rho}\bar{\mathbf{v}} \cdot \nabla_H \bar{q}_t\rangle$	LHF	$LF_p(0)$	$\bar{\rho} _h L w_e \Delta q_t$	$\bar{\mathbf{v}} _h \cdot \nabla_H h$	residual
15°N–35°N	-41 ± 20	112 ± 6	-11^{+6}_{-5}	-66^{+29}_{-31}	4	-3^{+44}_{-35}
25°N–35°N	-29 ± 20	89 ± 6	-3^{+6}_{-3}	-58^{+29}_{-33}	2	1^{+52}_{-35}
15°N–25°N	-54 ± 20	134 ± 6	-18 ± 6	-75 ± 29	6	-7 ± 36
30°N–35°N	-19	81	-1	-66	0	-6
25°N–30°N	-39	98	-6	-49	3	8
20°N–25°N	-56	124	-15	-75	8	-14
15°N–20°N	-51	145	-21	-75	3	1
CBW2005	-26 ± 7	99 ± 2	-5 ± 1	-68 ± 10		0

Second application of MAGIC data:

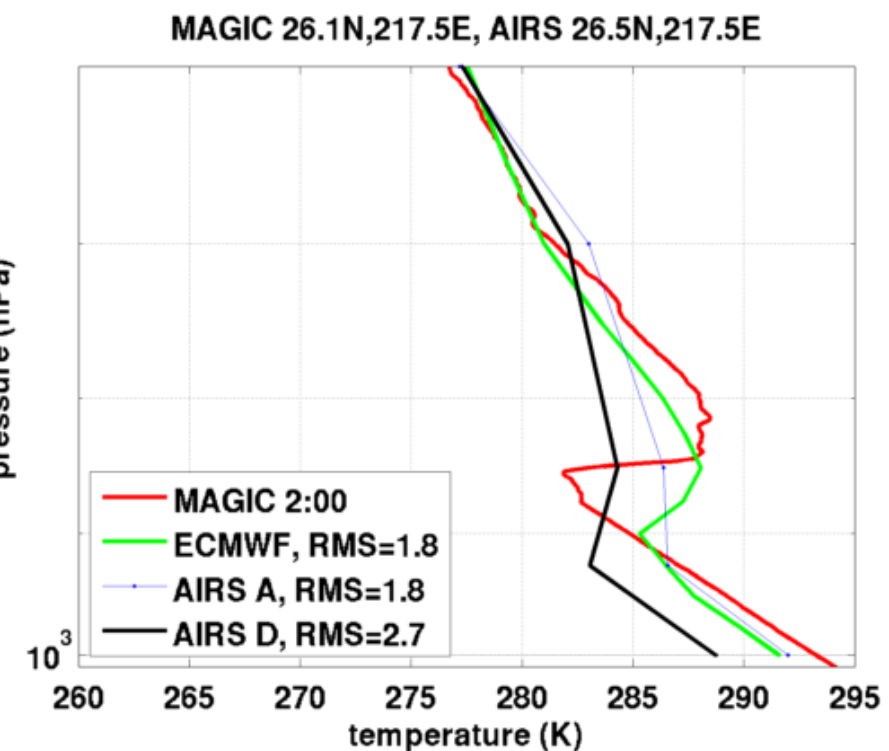
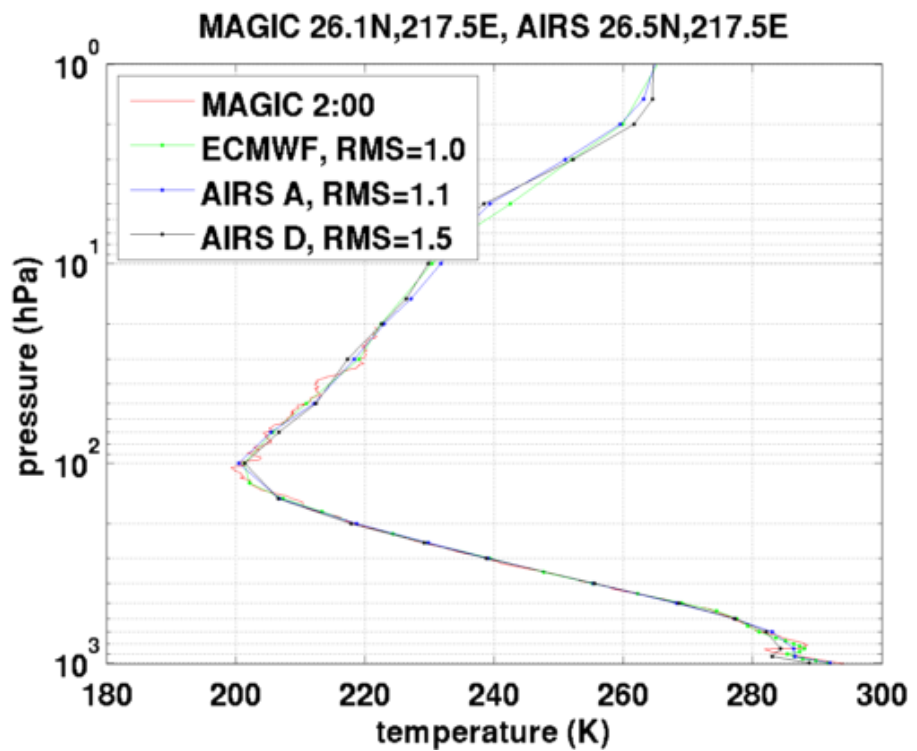
checking AIRS and ECMWF temperature and mixing ratio profiles
against MAGIC radiosondes

work in progress

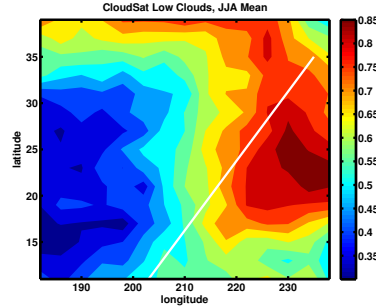
AIRS and ECMWF vs. MAGIC radiosondes



460 MAGIC soundings compared with AIRS and ECMWF



Conclusions



BL energy and water budgets close to 3 Wm^{-2} . We observe a gradual change between stratocumulus and cumulus regimes, involving rebalancing between most budget terms

Our understanding of uncertainties and errors on our data is still in early days
budget analyses highlight this, and may help

Observational budgets can provide a holistic picture of a region
this may prove useful for testing data and models

Ongoing and future work:

AIRS profile comparisons to MAGIC

higher precision budget analysis along MAGIC track (instead of GPCI)

SCM boundary layer parameterization tests against MAGIC data

I'm interested in the consolidated NAV data, and in the radar layer height VAP.